Food Chemistry: X 21 (2024) 101104

Contents lists available at ScienceDirect

Food Chemistry: X

journal homepage: www.sciencedirect.com/journal/food-chemistry-x

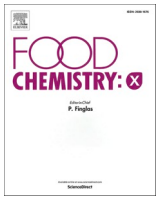

# Study on the thawing characteristics of beef in ultrasound combined with plasma-activated water

Huixin Wang [a], Changjiang Ding [a,b,*], Jingli Lu [a,*], Yuting Bao [a], Bingyang Han [a], Jie Zhang [a], Shanshan Duan [a], Zhiqing Song [a,b], Hao Chen [a]

[a] College of Science, Inner Mongolia University of Technology, Hohhot 010051, China
[b] Electric Power College, Inner Mongolia University of Technology, Hohhot 010051, China

ARTICLE INFO

*Keywords:*
Plasma-activated water
Thawing rate
Sterilization
Water holding capacity
Lipid oxidation

ABSTRACT

The effects of deionized water thawing (DT), plasma-activated water thawing (PT), ultrasound (150 W, 40 kHz) combined with deionized water thawing (UDT), and ultrasound combined with plasma-activated water thawing (UPT) on the thawing characteristics and the physicochemical properties of the beef were investigated. The results showed that the UPT group had a faster thawing rate (38 % higher compared to the PT group) and good bactericidal ability (75 % higher compared to the UDT group), and had no adverse effect on the color and pH value of the beef. Plasma-activated water (PAW) can maintain the stability of the beef fiber, improve the water holding capacity (WHC), inhibit lipid oxidation, and reduce the loss of soluble substances such as protein. Therefore, UPT thawing is a promising meat thawing technology, which provides practical guidance and methods for the wide application of UPT in the field of meat thawing.

## 1. Introduction

Beef is rich in protein, vitamins and minerals, with high nutritional value, loved by people. In recent years, with the improvement of the living standard of the population, the consumption of beef has also increased greatly, and at present, the per capita consumption of beef in the domestic meat is second only to pork.

Frozen storage is a widely used method in the preservation of meat and meat products. Low temperatures slow down the rate of biological and chemical reactions and inhibit the growth and metabolism of microorganisms, thus extending the shelf life of meat and meat products (Coombs, Holman, Friend, & Hopkins, 2017). Frozen foods must be thawed before any other subsequent food processing or cooking. The primary goal of thawing is to restore frozen meat to its fresh, unthawed condition and quality. Improper thawing can lead to undesirable changes in meat quality, such as deterioration of flavors, texture, color, protein degradation and aggregation. The time, temperature and method of the thawing process are the main factors affecting changes in the quality of thawed meat (Qian et al., 2019). It is important to note that neither freezing nor thawing can reduce the number of live microorganisms present in the meat. During the thawing process, dormant microorganisms in the frozen meat gradually regain their activity, and the exudates formed after thawing provide sufficient nutrients for the growth of microorganisms. Therefore, the thawing process of frozen meat products not only plays a vital role in their microbiological safety, but also affects the key quality attributes of the meat (Qian, Yan, Ying, Luo, Zhuang, & Yan, 2022).

The traditional thawing methods currently used are mainly air thawing and water thawing (Eastridge & Bowker, 2011). Air thawing uses air as the heat-conducting medium, which has lower production costs, but has the disadvantages of slow thawing speed and serious losses. Water thawing method, although faster, causes further microbial contamination of thawed meat due to prolonged immersion in water. In recent years, ultrasound thawing technology has received more and more attention due to its advantages of safety and environmental protection, uniform thawing, high efficiency and low cost (Kong et al., 2022). Ultrasound can effectively enhance various mass transfer processes unlike the traditional outside-in thawing method, both frozen and unfrozen tissues of food absorb the energy generated by ultrasound attenuation, with frozen tissues absorbing more energy than thawed tissues, thus significantly improving thawing efficiency (Tao et al., 2022). Ultrasound thawing is currently being used with excellent results in the application of fruit and vegetable (Forghani & Oh, 2013) and meat (Cao et al., 2010). In ultrasound thawing, deionized water is usually

* Corresponding authors.
*E-mail addresses:* ding9713@163.com (C. Ding), lujingli2004@163.com (J. Lu).

https://doi.org/10.1016/j.fochx.2023.101104
Received 21 November 2023; Received in revised form 20 December 2023; Accepted 25 December 2023
Available online 26 December 2023

used as the thawing medium. Liao et al. (2020) found that beef defrosted with PAW has higher quality than that defrosted with deionized water. So, PAW can replace deionized water as the new thawing medium.

Plasma is considered to be the fourth state of matter, which is an ionized gaseous mixture of active substances with antimicrobial effects. Plasma discharge can generate a large amount of RONS. By placing water under the plasma discharge environment, a large amount of RONS in the gas-phase plasma is transferred to the liquid, and physicochemical reactions with the water occur (Lu et al., 2008). In recent years, it has been found that PAW contains a large number of free radicals, reactive oxygen, reactive nitrogen and other components, which can effectively inactivate a variety of bacteria, such as *Salmonella, Staphylococcus aureus, Escherichia coli*, and other food spoilage bacteria and food-borne pathogenic bacteria. However, its research mainly focuses on the sterilization of fruits and vegetables by immersion, and is rarely applied to meat products (Ganesanet al., 2021).

Although there are some previous studies on the application of ultrasound-assisted thawing in meat products, there are few studies on ultrasound combined with plasma-activated water thawing. Therefore, this research uses plasma-activated water as the thawing medium and combined with ultrasound to thaw frozen beef. By exploring the basic characteristics of the thawed beef such as color, pH, water holding capacity (WHC), lipid oxidation, nitrite content and other basic characteristics, as well as analyses of bactericidal effect, protein loss, Fourier Infrared Spectroscopy (FTIR), and Scanning Electron Microscopy (SEM), the effect and law of ultrasound combined with plasma-activated water for beef thawing were investigated. This work investigated the thawing characteristics, physicochemical properties, and microstructure of frozen beef in ultrasound combined with plasma-activated water, which provides theoretical basis and experimental data for the application of

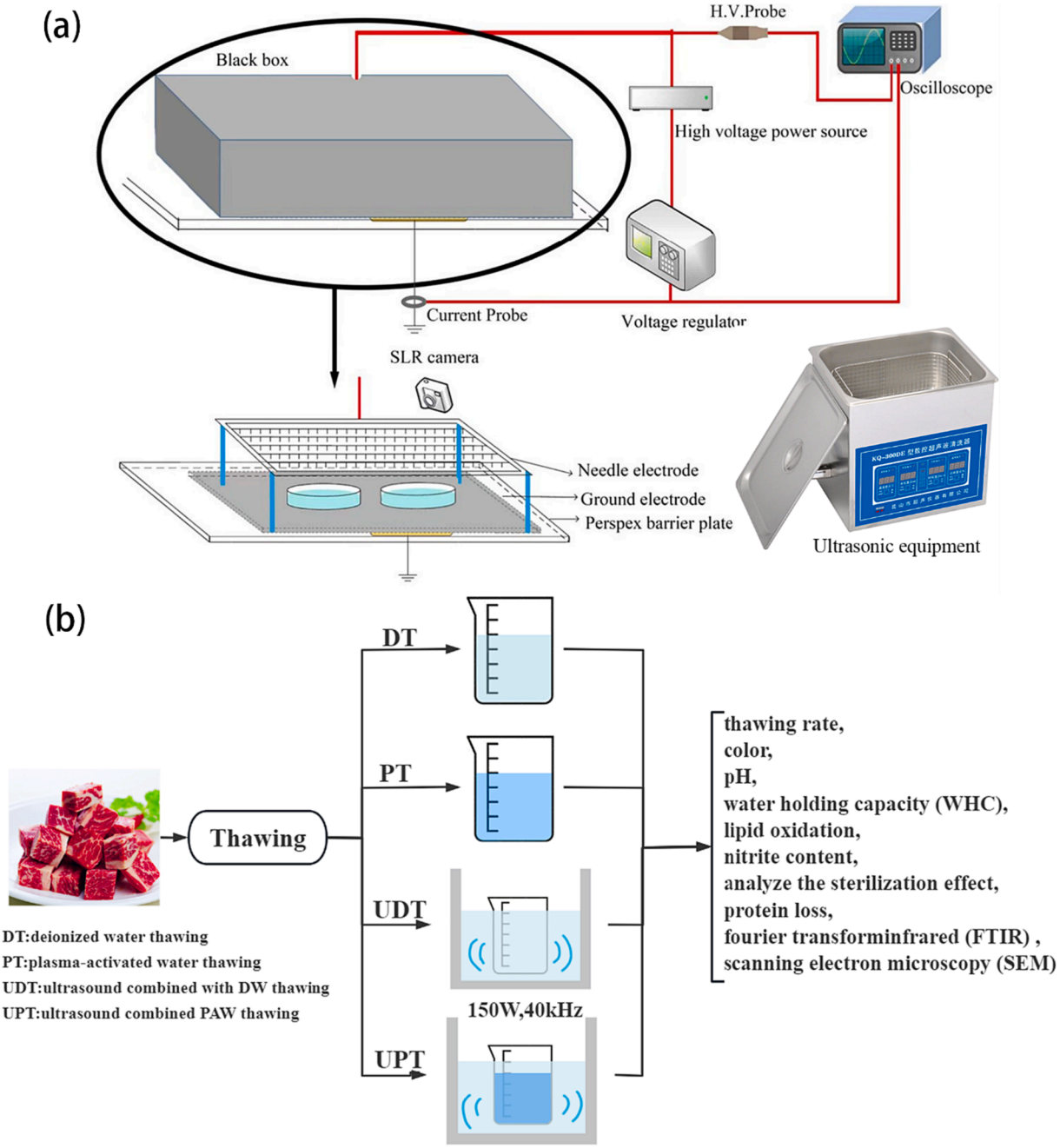


**Fig. 1.** Device for measuring dielectric barrier discharge characteristics (a) and experimental process (b).

ultrasound combined with plasma activated water in the field of meat thawing.

## 2. Materials and methods

### 2.1. Preparation of beef samples

Fresh beef was purchased from a local supermarket in Hohhot City, Inner Mongolia Autonomous Region. And the beef was supplied by a commercial slaughterhouse that processed cattle of the same breed and similar weight, raised for about one year and slaughtered on the same day. The fascia was removed, and the beef was cut into square samples of 35 mm × 30 mm × 30 mm in the direction of muscle texture, weighing about 30 ± 1 g. The beef was then frozen in a refrigerator at −20 °C for 24 h. All samples were processed under the same conditions, and different thawing treatments were randomly selected to eliminate the errors caused by ice crystals as much as possible.

### 2.2. Preparation of PAW

In this paper, according to the PAW preparation method of Li et al. (2022), a needle array-plate dielectric barrier discharge device (KZX-2–1.5KVA, Wuhan High Voltage Electric Appliance Factory) was used (Fig. 1a). The power supply of the experimental device was AC, the frequency was 50 Hz, and the voltage was continu-ously adjustable from 0 to 50 kV. The high-voltage electrode was composed of an array of needles (14 × 7 needles) with a length of 20 mm, a diameter of 1.5 mm, a radius of curvature of 0.75 mm, and a horizontal and vertical spacing of 4 cm. The electrode (85 × 45 $cm^2$) of the stainless steel was ground, and a 4 mm-thick Plexiglas plate (100 × 60 $cm^2$) was placed between the ground electrode and material. A dark box was used to enclose the entire electrode system to create a relatively closed experimental environment. During the plasma discharge process, air was allowed to enter to effectively reduce the loss of discharge plasma to the outside by diffusion and thus maintain a more obvious plasma effect.

150 mL of deionized water was placed into a polypropylene petri dish with an inner diameter of 14 cm and activated using a voltage of 25 kV and a needle-media-plate distance of 4 cm for 60 min. The treated activated water was then left to stand until room temperature (20 °C), which was held constant by an air conditioner. A portion of the activated water was collected to measure the initial pH, conductivity, and nitrite content before thawing. This process lasts for approximately 10 min.

The ultrasound system (KQ-300DE, Kunshan) consisted of an ultrasound generator, a treatment chamber and a control system. The water temperature of the ultrasound generator was controlled at room temperature of 20 °C, the power was controlled at 150 W, and the ultrasound operating frequency was 40 kHz (Zhang et al., 2018).

### 2.3. Thawing process

The frozen beef was thawed using deionized water thawing (DT), plasma-activated water thawing (PT), ultrasound combined with deionized water thawing (UDT), and ultrasound combined with plasma-activated water thawing (UPT), respectively, by taking 100 mL of deionized water as well as activated water in a 200 mL beaker (Fig. 1b). Due to the complex composition of tap water, in order to ensure experimental rigor and reduce experimental errors, this study referred to the methods of Qian et al. (2022) and Kong et al. (2022), and used deionized water as thawing medium. A digital temperature sensor (NTC, Guangdong) was inserted into the geometric center of the beef to record the beef center temperature until the beef center temperature reached 4 °C, and the center temperature was recorded every 1 min during the thawing process. Any three beef samples in each group were selected for the thawing experiment, which was repeated at least three times.

### 2.4. Microbiological analyses

5 g of thawed beef sample was placed in 45 mL of 0.85 % sterile physiological saline for homogenization. Then, the mixture and the thawed medium were collected after homogenization, continuously diluted 10 times to the appropriate concentration, and analyzed on PCA (Plate count agar, for the total bacterial) agar (Qian et al., 2022). The number of colonies was recorded after 48 h of incubation in a 37 °C thermostat (MJ-500-II, Shanghai), and the results were expressed as $\log_{10}$UFC/g for samples and $\log_{10}$UFC/mL for media.

### 2.5. Water holding capacity

#### 2.5.1. Drip loss

Referring to the method of Hsieh et al. (2010), 3 samples of each treatment were quickly weighed before thawing and then re-weighed after thawing to calculate the drip loss rate of beef using the following equation:

$$D = \frac{(m_1 - m_2)}{m_1} \times 100\% \quad (2\text{-}1)$$

where $D$ is the drip loss rate of beef, $m_1$ is the mass of beef before thawing (g), and $m_2$ is the mass of beef after thawing (g).

#### 2.5.2. Cooking loss

Referring to the method of Pang et al. (2020), 20 g of thawed beef was taken and placed in a constant temperature water bath (HH-4, China) at 95 °C for 30 min. The mass of the beef samples was weighed before and after steaming and the rate of steaming loss of beef was calculated using the following equation:

$$C = \left(\frac{m_x - m_y}{m_x}\right) \times 100\% \quad (2\text{-}2)$$

where $C$ is the cooking loss rate of beef, $m_x$ is the mass of beef (g) before cooking and $m_y$ is the mass of beef (g) after cooking.

#### 2.5.3. Centrifugal loss

Referring to the method of Bian et al. (2022), 10 g sample of minced meat was taken in a 10 mL tube and centrifuged at 10000 × g for 20 min at 4 °C, the liquid in the test tube was removed and the meat sample was weighed again. The percentage of water loss was recorded as centrifugal loss. The following formula was used to calculate the centrifugal loss of beef:

$$Ce = \frac{m_b - m_a}{m_b} \times 100\% \quad (2\text{-}3)$$

where $Ce$ is the centrifugal loss rate of the beef, $m_a$ is the mass of beef (g) after centrifugation and $m_b$ is the mass of beef (g) before centrifugation.

### 2.6. Color and pH

Using a fully automated colorimeter (3nh-NR60CP, LED illumination, CIE standard illuminance D65, 10° observer, 8 mm diameter aperture, Shenzhen), the color parameters of the beef samples were determined by measuring $L^*$ (lightness), $a^*$ (redness) and $b^*$ (yellowness) on the surface of the beef samples before and after thawing, respectively. Measurements were repeated five times for each sample, and the average value was calculated as the experimental result. The color difference ΔE of the sample was calculated as follows (Bian et al., 2022):

$$\Delta E = \sqrt{(L_1 - L_0)^2 + (a_1 - a_0)^2 + (b_1 - b_0)^2} \quad (2\text{-}4)$$

where $L_0$, $a_0$, $b_0$ and $L_1$, $a_1$, $b_1$ denote the lightness, redness and yellowness of beef before and after thawing, respectively.

For the pH value, 5 g of beef samples were cut into pieces, and 20 mL of deionized water was added to achieve full homogenization. And the pH value of the mixture as well as of the thawed medium was measured using a pH meter (SevenCompact™, Switzerland), which needed to be calibrated before each use (Liu et al., 2013).

### 2.7. Lipid oxidation

Malondialdehyde was measured in beef using the Malondialdehyde Test Kit (Solarbio, China). Oxygen free radicals act on the unsaturated fatty acids of lipids to produce lipid peroxidation, which gradually breaks down into a series of complex compounds including MDA, the level of which can be detected as a function of lipid oxidation by measuring the level of MDA, which condenses with thiobarbituric acid (TBA) to form a red color product with a maximum peak at 532 nm, which can be used to estimate the level of lipid peroxidation in the sample after colorimetry. After colorimetry, the content of lipid peroxide in the sample can be estimated. At the same time, the absorbance at 600 nm was measured, and the difference between the absorbance at 532 nm and 600 nm was used to calculate the content of MDA.

$$MDA\ \text{content} = 32.258 \times \Delta A\tilde{A} \cdot W \tag{2-5}$$

$$\Delta A = \Delta A532 - \Delta A600 \tag{2-6}$$

where $W$ is the sample mass, $\Delta A532$ is the sample absorbance at 532 nm, and $\Delta A600$ is the sample absorbance at 600 nm.

### 2.8. Nitrite determination

According to < GB 5009.33–2016 National Standard for Food Safety Determination of Nitrite and Nitrate in Foods>, weigh 5 g of beef samples in a 500 mL beaker, add 12.5 mL of saturated borax solution (50 g/L), add deionized water to 150 mL, and shake at 150 °C, then heated in a boiling water bath for 15 min, taken out and placed in cold water to cool down and placed to room temperature. Subsequently, potassium ferricyanide solution (106 g/L) and zinc acetate solution (220 g/L) were added with 5 mL each and shaken well to precipitate the protein. The supernatant was filtered through filter paper (FT-3–104-110, 110 mm, Sartorius) with strong water absorption, and 30 mL of the initial filtrate was discarded. Forty milliliters of the filtrate are placed into a 50 mL stoppered cuvette, and 2 mL of p-aminobenzenesulfonic acid solution (1 %, w/v) was added, mixed well and left for 5 min. Then, 1 mL of N-1-naphthyl ethylenediamine solution (0.1 %, w/v) was added, and water was added to the desired volume, mixed well and left for 15 min. The nitrite content was determined by UV–vis absorption spectrometry at 540 nm according to a standard curve. (The reagents and solutions used in this experiment are from Tianjin Xinbute Chemical Co.).

For nitrite in the medium, the same 40 mL of medium was taken in a 50 mL stoppered cuvette, 2 mL of p-aminobenzene sulfonic acid solution (1 %, w/v) was added, mixed well, and left to stand for 5 min. 1 mL of N-1-naphthalene ethylenediamine solution (0.1 %, w/v) was added. Water was added to the scale, mixed well, and left to stand for 15 min, and then the content of nitrite was determined according to the standard curve.

$$Nitritecontent = 0.0208 \times \Delta A540 + 0.0002 \tag{2-7}$$

where $\Delta A540$ is the sample absorbance at 540 nm.

### 2.9. Protein loss

In order to evaluate the protein loss of beef after thawing treatment under different conditions, the protein concentration in the thawing medium was determined. The protein concentration was determined using the BCA method. The BCA protein quantification kit (PA115, Tengen Biotechnology (Beijing) Co. Ltd.) was used according to the instructions (Vinarov, Lytle, Peterson, Tyler, Volkman, & Markley, 2004).

### 2.10. Fourier infrared spectroscopy (FTIR) and protein secondary structure determination

According to the operation manual of FTIR spectrometer (IRTracer-100, Japan), the thawed beef samples were dried in an oven at 40 °C and ground into powder, and the powder was mixed with potassium bromide in the ratio of 1:100 and ground again. The powder was mixed with potassium bromide in the ratio of 1:100 and ground again. The samples were pressed using a HY-12 tablet press, and then placed into an FTIR spectrometer to scan the samples in the range of 400–4000 $cm^{-1}$. The resulting curves were processed to remove the interference peaks of moisture and carbon dioxide to obtain the infrared spectra of the beef after thawing.

The amide I band in the IR spectra is mainly used for protein assignment of secondary structure (Carbonaro, Maselli, & Nucara, 2012). The percentage of α-helix, β-sheet, β-turn, β-antiparallel and random coil in the composition of protein secondary structure was calculated using Peak Fit v4.12 by selecting the 1600–1700 $cm^{-1}$ bands of the infrared spectra for back-integration, second-order derivation, and curve fitting.

### 2.12. Scanning electron microscopy (SEM)

Thawed beef samples were placed in 2.5 % glutaraldehyde and then fixed in a refrigerator at 4 °C for 24 h according to the operating manual of the scanning electron microscope (S3400, Japan). After removal of the glutaraldehyde buffer, the samples were critical point dried using gradually increasing concentrations of ethanol (50–100 %) and propylene oxide (100 %), and finally sprayed with gold, and the samples were scanned with a scanning electron microscope after 60 s to observe the microstructure of the beef samples (Li et al., 2020).

### 2.13. Statistical analyses

Graphing was performed using Origin software and each group of experiments was independently repeated three times and the results were expressed as mean ± standard deviation (SD). Statistical analyses were performed using SPSS software, and statistically significant differences in the results were determined by one-way analysis of variance (ANOVA) and Duncan's multiple range test. The level of statistical significance is expressed as p-value ($p < 0.05$ indicates a significant difference).

## 3. Results and discussion

### 3.1. Thawing center temperature

Fig. 2 shows the thawing curves and thawing rates of beef under different conditions, in which it can be seen that the average thawing rate was significantly increased and the thawing time was significantly reduced after combined ultrasound ($p < 0.05$). In order to explore the effect of ultrasound waves on the thawing process in more detail, the change of beef temperature during the thawing process was monitored by the central temperature, and it could be seen that the whole thawing process was divided into three stages: the first stage was from −20 °C to −5 °C, the second stage was from −5 °C to −1 °C, and the third stage was from −1 °C to 4 °C. There was no significant difference in the thawing time between the first and third stages, but the main effect occurred in the second stage, which was called the " Maximum ice crystal generation zone"(Xu et al., 2015), and the addition of ultrasound significantly shortened the time in the second stage ($p < 0.05$). The reason for the accelerated thawing by ultrasound is, on the one hand, due to the cavitation effect, when the ultrasound power reaches a certain intensity,

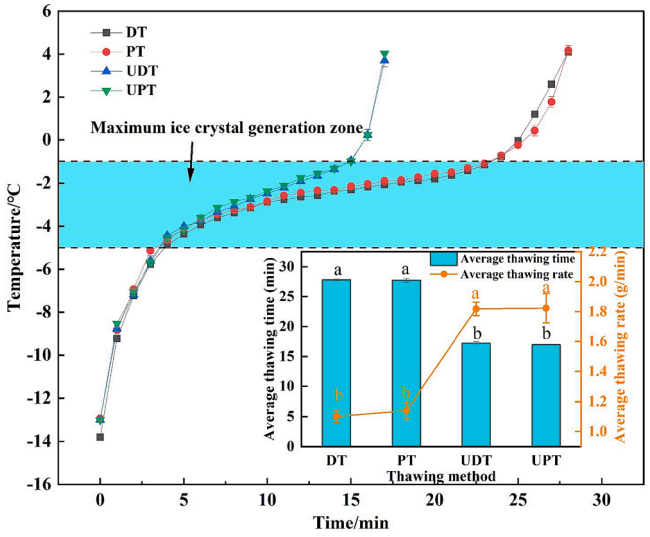


**Fig. 2.** Center temperature profile and thawing time of beef under different thawing conditions. **Note:** Different letters indicate significant differences in the results ($p < 0.05$). DT: deionized water thawing; PT: plasma-activated water thawing; UDT: ultrasound combined with deionized water thawing; UPT: ultrasound combined with plasma-activated water thawing.

small holes will appear in the structure of the frozen material, which will cause the frozen state of the material to be disintegrated microscopically. On the other hand, the micro-jet and turbulence produced by the thawed drip under the action of ultrasound will also help to transfer the heat and the dissolution of the ice crystals (Cai et al., 2019).

### 3.2. Microbiological analyses

Fig. 3(a) and (b) show the total number of viable bacteria in beef samples and media after thawing in different ways. The total number of viable bacteria in beef samples after DT, PT, UDT, and UPT treatments were 4.46 ± 0.009, 3.866 ± 0.027, 4.11 ± 0.008, and 3.54 ± 0.020 $\log_{10}$CFU/g, respectively, and the total number of colonies in the media were 3.85 ± 0.005, 1.66 ± 0.083, 3.52 ± 0.013, and 1.50 ± 0.142 $\log_{10}$CFU/ml. Compared with DT, the use of plasma-activated water thawing and combined ultrasound thawing significantly reduced bacterial colonies in both beef samples and thawing media. The UPT treatment had the best bactericidal effect on bacteria, followed by the PT group, indicating that the PAW has good bactericidal effect. < China's National Hygiene Standard GB/T 9959.2–2008 > stipulates that the total number of bacterial colonies in fresh and frozen pork should not exceed 6 $\log_{10}$CFU/g. Rossow et al. (2018) found a decrease in bacterial count of 0.78–2.55 CFU/cm$^2$ in chicken breast meat treated with PAW. Gambuteanu et al. (2013) found that the number of aerobic microorganisms in the longissimus dorsi muscle of pigs decreased by about 11 % compared to still water thawing after thawing using ultrasound at 25 kHz, 0.2–0.4 W/cm$^2$. This is because during the generation of PAW, a large amount of key substances such as ROS and RNS are produced, and the bactericidal effect of PAW depends on the composition and concentration of RONS, which is capable of breaking the molecular structure of peptidoglycan, leading to the rupture of the bacterial cell wall, thus causing oxidative stress in the cell membrane, altering the surface structure and chemical state of bacteria, and entering the cell to destroy proteins, leading to DNA decomposition and damage to other internal components, thus providing a sterilizing effect (Royintarat & Seesuriyachan, 2019). After combined ultrasound, the number of colonies is further reduced, indicating that ultrasound also has a certain effect on the inactivation of bacteria, which is the use of ultrasound cavitation produced by ultrahigh pressure can make microbial cell fragmentation, thereby inactivating microorganisms and inhibiting the growth of microorganisms (Becton et al., 2017). Therefore, ultrasound combined with plasma-activated water can inhibit the growth and reproduction of microorganisms, prolong the shelf life of meat samples and improve their quality.

### 3.3. Water holding capacity (WHC)

The water holding capacity of meat not only affects the taste, aroma, juiciness, nutrients, tenderness, color and other edible qualities of meat, but also directly affects the yield of meat products, which has an important economic value, and lower WHC means a greater economic loss for the meat industry. Table 1 demonstrates the drip loss, cooking loss and centrifugation loss of beef after thawing under different conditions. Both cooking loss and centrifugation loss were significantly lower in experimental group than in DT group and PT group had the smallest cooking loss of 39.97 ± 0.81 % as well as the smallest centrifugation loss of 16.62 ± 1.31 %. Qian et al. (2022) found that both PAW and ultrasounds improved WHC of chicken meat. Islam et al. (2014) investigated the effect of ultrasounds on the quality of mushrooms and reported that ultrasounds (0.39 W cm$^2$, 20 kHz) increased WHC by 10 %. Zhang et al. (2018) treated porcine longissimus muscles with ultrasound at different power levels and found that the WHC of the meat decreased and then increased with increasing power, with the best WHC at 180 W. The WHC is closely related to the electrostatic charge number of myofibrillar proteins and the reticular structure of proteins. The electrostatic charge in protein molecules has the effect of attracting water molecules. At the same time, the electrostatic charge can enhance the electrostatic repulsive force between protein molecules, making their structure loose and water retention, while when the electrostatic charge decreases, the repulsive force decreases, the protein molecules are aggregated together, and the water holding capacity decreases (Huff-Lonergan & Lonergan, 2005). PAW contains a large number of positive and negative ions, prompting the enhancement of the electrostatic charge effect of proteins with the formation of network structure, which is conducive to water retention. Whereas the WHC of beef was reduced after combined ultrasound, this may be due to the fact that the meat tissue cells were affected by the mechanical or cavitation effect of ultrasound, which made the muscle fibers and intramuscular membrane separated, increased the cell gap, and the compactness of the muscle tissue was reduced (Sriket et al., 2007). Drip loss was significantly higher ($p < 0.05$) in all experimental groups than in DT. During thawing, ice melting in the extracellular space may re-flow into the intracellular space, which is subsequently reabsorbed by dehydrated fibers and denatured proteins. The electrostatic repulsion between protein molecules was enhanced by electrostatic charging in the PAW, which resulted in the failure of extracellular water to enter into the cell smoothly, leading to the higher loss of drips (Zhang et al., 2019). In the case of the UDT group, it was due to a shorter thawing time, which did not allow sufficient time for extracellular water to enter the cell, resulting in a higher drip loss (Huff-Lonergan et al., 2005).

### 3.4. Color and pH

The pH value is an important indicator that can affect indicators such as meat color and cooking loss (Kong et al., 2022). Fig. 3(c) shows the changes in pH value before and after thawing of thawing media under different conditions, PAW resulted in a low pH value due to the presence of a large amount of active substances. After thawing, the pH values of the DT and UDT groups decreased, most likely due to the loss of minerals and small-molecule proteins from the meat by exudation during the thawing process, which led to a change in the ionic balance, thus lowering the pH value (Leygonie, Britz, & Hoffman, 2012b). Whereas, the increase in pH value in the PT and UPT groups further indicates that the active substances were consumed for a number of reactions such as sterilization. Due to glycolysis, acidic substances produced in the muscle may lead to a decrease in pH value during the thawing process.

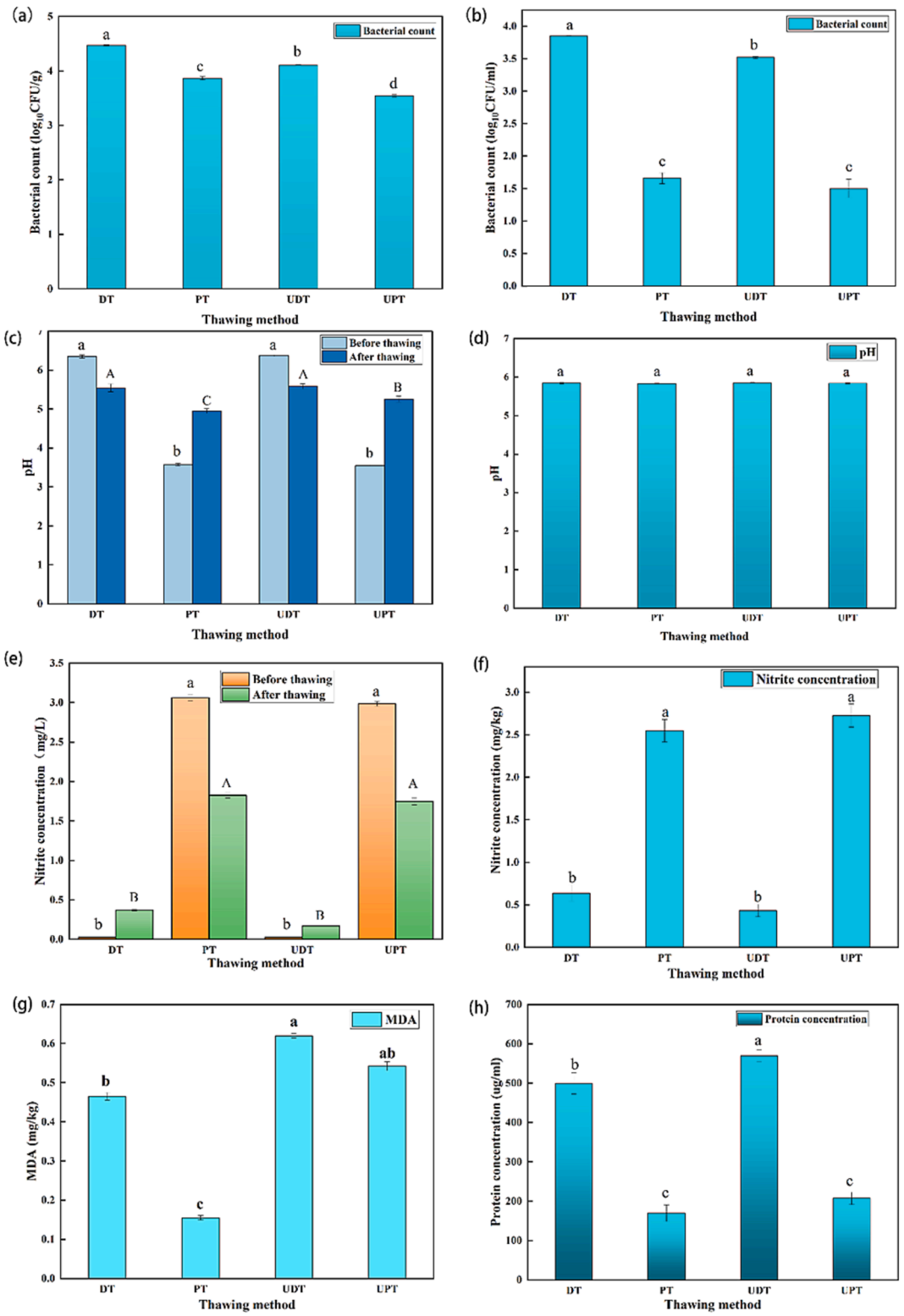


**Fig. 3.** Total number of viable bacteria in beef samples (a) and thawing media (b) after different thawing treatments; pH of thawing media (c) and beef samples (d) before and after thawing; $NO_2$content of thawing media (e) and beef samples (f) before and after thawing; MDA content of beef after thawing (g); and protein content of thawing media (h). **Note:** Different letters indicate significant differences in the results ($p < 0.05$). DT: deionized water thawing; PT: plasma-activated water thawing; UDT: ultrasound combined with deionized water thawing; UPT: ultrasound combined with plasma-activated water thawing.

Conversely, nitrogen-containing substances are broken down into alkaline substances, leading to an increase in pH value (Liu et al., 2013). In Fig. 3(d), the difference in pH value among the groups was not statistically significant ($p > 0.05$), indicating that PAW as well as ultrasound treatment did not negatively affect beef pH value. This is consistent with the results of previous studies (Kong et al., 2022).

Color has a significant impact on the appearance and acceptability of frozen products. Table 2 demonstrates the color changes of beef before

**Table 1**
Drip loss, cooking loss and centrifuge loss of beef after thawing under different conditions.

| | DT | PT | UDT | UPT |
|---|---|---|---|---|
| *Drip loss %* | $2.27 \pm 0.70^{c}$ | $3.17 \pm 0.38^{b}$ | $3.99 \pm 1.46^{a}$ | $3.34 \pm 0.01^{ab}$ |
| *Cooking loss %* | $42.61 \pm 0.68^{a}$ | $39.97 \pm 0.81^{c}$ | $41.75 \pm 0.77^{b}$ | $41.59 \pm 1.16^{b}$ |
| *Centrifuge loss %* | $18.10 \pm 1.57^{a}$ | $16.62 \pm 1.31^{c}$ | $17.22 \pm 1.17^{b}$ | $17.49 \pm 2.67^{b}$ |

**Note:** Values are the mean of triplicate measurements ± standard deviation. Different letters indicate significant differences in the results ($p < 0.05$). DT: deionized water thawing; PT: plasma-activated water thawing; UDT: ultrasound combined with deionized water thawing; UPT: ultrasound combined with plasma-activated water thawing.

**Table 2**
Color change of beef after thawing under different conditions.

| | DT | PT | UDT | UPT |
|---|---|---|---|---|
| $L_0$ | $41.28 \pm 1.00^{aA}$ | $42.13 \pm 1.08^{aA}$ | $41.08 \pm 0.60^{aA}$ | $41.35 \pm 0.45^{aA}$ |
| $L_1$ | $49.24 \pm 1.09^{aB}$ | $49.22 \pm 0.79^{aB}$ | $48.93 \pm 0.46^{aB}$ | $48.74 \pm 0.34^{aB}$ |
| $a_0$ | $17.49 \pm 0.38^{aA}$ | $17.40 \pm 0.30^{aA}$ | $17.57 \pm 0.24^{aA}$ | $17.69 \pm 0.43^{aA}$ |
| $a_1$ | $14.46 \pm 0.82^{bB}$ | $15.78 \pm 0.28^{aB}$ | $14.55 \pm 1.31^{aB}$ | $15.67 \pm 0.54^{bB}$ |
| $b_0$ | $15.76 \pm 0.71^{aA}$ | $15.49 \pm 0.68^{aA}$ | $15.52 \pm 0.21^{aA}$ | $15.37 \pm 0.54^{aA}$ |
| $b_1$ | $13.13 \pm 0.49^{aB}$ | $12.78 \pm 0.54^{aB}$ | $13.22 \pm 0.16^{aB}$ | $12.63 \pm 0.73^{aB}$ |
| $\Delta E$ | $8.9 \pm 0.97^{a}$ | $7.76 \pm 0.71^{b}$ | $8.66 \pm 0.4^{b}$ | $7.85 \pm 0.27^{b}$ |

**Note:** Values are the mean of triplicate measurements ± standard deviation. Mean values with different lowercase letters ($^{a, b, c}$) indicate significant differences among different thawing methods, different capital letters ($^{A, B}$) indicate a significant difference in the color of the beef before thawing and after thawing ($p < 0.05$). where $L_0$, $a_0$, and $b_0$ indicate the brightness, redness and yellowness of the beef before thawing, respectively, and $L_1$, $a_1$, and $b_1$ indicate these parameters after thawing, respectively. DT: deionized water thawing; PT: plasma-activated water thawing; UDT: ultrasound combined with deionized water thawing; UPT: ultrasound combined with plasma-activated water thawing.

and after thawing under different conditions. The $L^*$ of all groups increased significantly *($p < 0.05$)* after thawing, but there was no significant difference *($p > 0.05$)* among the groups. Higher $L^*$ imply that more in-meat water appeared on the surface of the meat in order to reflect the light and increase the brightness (Xu, Tian, Ma, Liu, & Zhang, 2016). Beef is a red meat, so the red color represents the freshness of the beef to some extent, for the a-value, the PT and UPT groups were significantly higher than the DT and UDT groups, the change in a-value was attributed to the accumulation of myoglobin and methemoglobin in the meat, and the degradation of haemoglobin due to the oxidation of the meat during thawing resulted in the decrease of the a-value (Xu et al., 2016). Nitrite, as a meat color protection agent, reacts with myoglobin in meat to form nitrosomyoglobin, which enhances the color of the meat, as well as the flavors and preservative properties of the meat (Jo et al., 2020). Fig. 3(e) shows the $NO_2^-$content of thawing medium before and after thawing, after thawing, the nitrite in the meat of DT and UDT groups entered into the medium through diffusion, which led to an increase in the nitrite content of the medium. The $NO_2^-$ in the medium of both PT and UPT groups decreased, and it can be seen through Fig. 3(f) that $NO_2^-$ content of beef samples of the PT and UPT groups was significantly higher than that of the rest of the two groups *($p < 0.05$)*, which indicates the transfer of nitrite from the medium to the meat and did not exceed the required nitrite content of 4.5 mg/kg in fresh meat products (Jo et al., 2020). This resulted in significantly higher a-values for beef samples in PT and UPT groups than in DT and UDT groups. As for the b values, no significant difference was shown among the groups *($p > 0.05$)*. ΔE reflected the total color change of the meat, and the ΔE values of the PT and UPT groups were significantly lower than those of the DT and UDT groups *($p < 0.05$)*, which indicated that the PAW had an effect on the retention of the beef color. The result of the research was similar to ours as shown in the research by Stadnik et al (2011).

### 3.5. Lipid oxidation

Lipid oxidation leads to deterioration of flavors, color, scent, quality and nutritional value of meat. As shown in Fig. 3(g), it demonstrates the MDA content in beef samples after thawing under different experimental conditions. Beef samples from the PT group contained the least amount of MDA at 0.15 ± 0.01 mg/kg. This is because beef is rich in heme myoglobin and haemoglobin, and the destruction of these haemoglobin moieties produces a large amount of free iron, which promotes the generation of reactive oxygen species, which play a catalytic role in lipid oxidation. PAW contains large amounts of nitrite, which binds to haemoglobin and myoglobin to form nitrosohaemoglobin and nitrosomyoglobin, which form stable compounds that reduce iron utilisation, thus inhibiting lipid oxidation (Dominguez et al., 2019). Herianto et al. (2022) suggested that PAW inhibited the growth of peroxidation-inducing microorganisms, thereby inhibiting MDA production. Chaijan et al. (2021) also found that PAW inhibited lipid oxidation by treating Asian sea bass with PAW. The degree of lipid oxidation was promoted by combined ultrasound, whose mechanical vibrations in the medium disrupted the integrity of the beef tissue (Sriket et al., 2007). In the thawing process, ultrasound led to the release of oxidative enzymes and prooxidants in the cellular organelles, and weakened the role of reducing agent. For ultrasound combined with plasma-activated water treatment accelerated the lipid oxidation of chicken, suggesting that the antioxidant enzymes remaining in chicken cannot defend against the action of reactive species in PAW when the integrity of chicken tissue was destroyed by ultrasound (Qian et al., 2022). Wang et al. (2022) and Li et al. (2023) similarly found that ultrasound thawing promotes lipid oxidation. But there are also some studies that ultrasound can inhibit lipid oxidation (Cai et al., 2020; Gan et al., 2022), for which more in-depth research may be needed.

### 3.6. Protein loss and SEM

As shown in Fig. 4, the microstructure of the fiber structure of beef after thawing under different experimental conditions, we performed longitudinal cutting of muscle fibers to determine the microstructure and assess the fiber gaps. It can be seen that after DT treatment, some of the fiber structure of beef was disrupted, with obvious fractures and increased inter-fiber gaps. Whereas, after PT treatment, beef fibers were relatively intact and dense without obvious cracks, which was attributed to the fact that PAW contained a large number of positive and negative ions, and the charge of these ions increased the electrostatic repulsion between the myogenic fibers of the thawed beef, inducing the expansion of myogenic fibers and maintaining the integrity of the muscle fiber tissue structure (Stadnik et al., 2008). And after combined ultrasound, more gaps appeared in the beef fibers of the UDT group due to the mechanical vibration of ultrasound, and the structure was loosened (Sriket et al., 2007). In contrast, in the UPT group, the fiber structure was not severely ruptured due to the presence of PAW. The disruption of beef fibers and the appearance of gaps leads to the loss of protein-based soluble substances within the meat. Fig. 3(h) shows the protein concentration in the media after thawing under different experimental conditions. It is in general agreement with the results of microstructural analysis. These results are consistent with the findings of Qian et al (2022).

### 3.7. Protein analysis

Fig. 5(a) shows the overlapped FTIR spectra of beef after thawing under different thawing conditions, and a total of seven characteristic peaks were obtained. After reviewing the data(Candoğan, Altuntas, & İğci, 2020), it was found that: the transmission peak near 1239.4 $cm^{-1}$ was attributed to $PO_2^-$asymmetric stretching; the characteristic peak near 1392.93 $cm^{-1}$ was attributed to COO-symmetric stretching; and the characteristic peak near 1545.02 $cm^{-1}$ was attributed to amide II; the

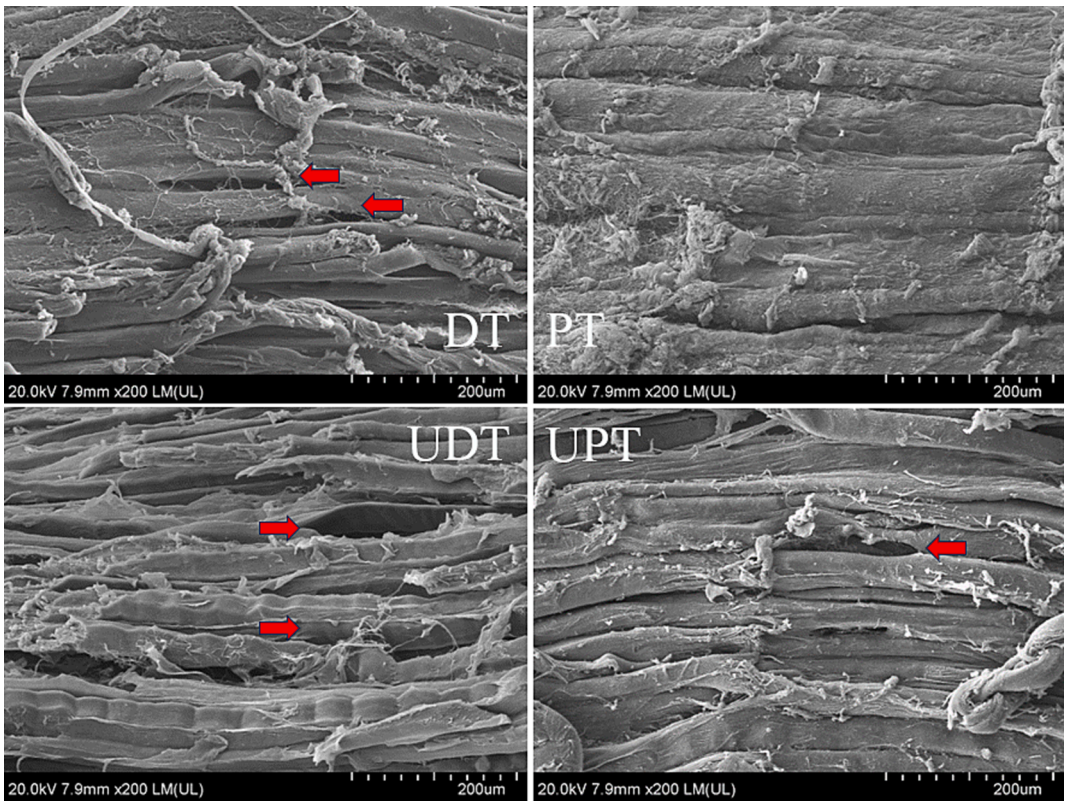


**Fig. 4.** Microstructure of fibre structure of beef after thawing under different thawing conditions (magnification: 200 × ). **Note:** DT: deionized water thawing; PT: plasma-activated water thawing; UDT: ultrasound combined with deionized water thawing; UPT: ultrasound combined with plasma-activated water thawing.

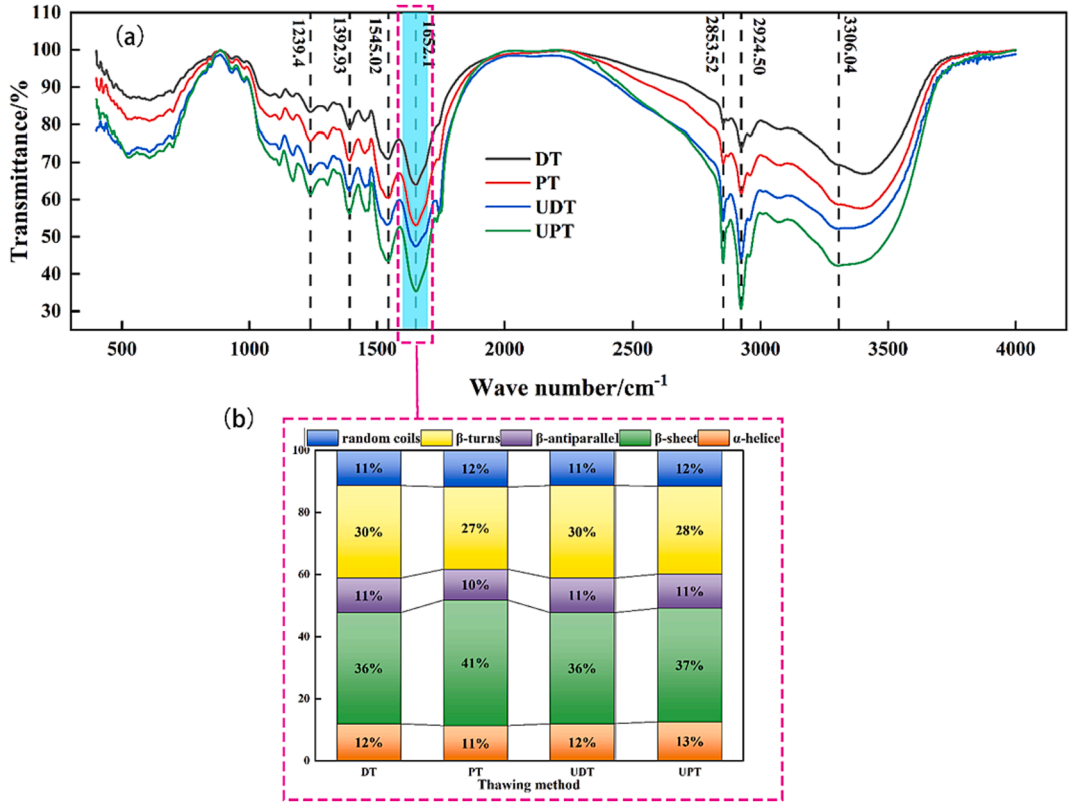


**Fig. 5.** Protein analysis. (a)Infrared spectra of beef thawed under different conditions, (b)Relative content of protein secondary structure. **Note:** DT: deionized water thawing; PT: plasma-activated water thawing; UDT: ultrasound combined with deionized water thawing; UPT: ultrasound combined with plasma-activated water thawing.

characteristic peak near 1652.10 $cm^{-1}$ is attributed to amide I; the characteristic peak near 2853.52 $cm^{-1}$ is attributed to $CH_2$-symmetric stretching; the characteristic peak near 2924.50 $cm^{-1}$ is attributed to $CH_2$ asymmetric stretching; and the characteristic peaks near 3306.04 $cm^{-1}$ are attributed to the N—H stretching of proteins and the O—H stretching of polysaccharides. As can be seen from the Fig. 5(a), the positions of the characteristic peaks in the IR spectra of beef thawed under different conditions are basically the same and no new characteristic peaks appeared, which suggests that the protein patterns after PAW and ultrasound treatments do not change and do not lead to the formation of new bonds. This is consistent with the previous research by Qian et al (2022). However, the intensity of transmission peaks was different, the higher the transmittance (vertical axis) value, the more light passes through the sample, indicating that the functional group has a lower content in the sample (Han et al., 2023). Compared with the DT group, the use of plasma-activated water and ultrasound both resulted in lower transmission peak intensities, with the UPT group having the lowest transmission peak intensities, followed by the UDT and PT groups, suggesting that ultrasound combined with plasma-activated water treatment can better retain the compounds and functional groups in the beef, preserving the nutrients to a greater extent, and improving the water retention capacity of the beef. The protein secondary structure content was obtained by using Peak fit v4.12 software for the 1600–1700 $cm^{-1}$ band of the infrared spectra with back integration, second-order derivation and curve fitting (Fig. 5(b)). Protein secondary structures can be divided into ordered and disordered structures. α-helices and β-sheets (parallel and antiparallel) are representatives of ordered structures. β-turns and random coils are representatives of disordered structures. In the figure, it can be seen that the PT group has the most ordered structure, followed by the UPT group, while the DT group and UDT group are almost identical. This may be due to the fact that α-helices and β-sheets are maintained by hydrogen bonding between peptide chains, which is the main force that stabilizes the secondary structure (Zhang et al., 2017), and reactive substances in PAW can reinforce the hydrogen bonding, resulting in a more stable protein structure. Kong et al. (2022) found that ultrasound-assisted slightly acidic electrolyzed water thawing had a more stable protein structure. Li et al. (2020) pointed out that the α-helix decreased with the increase of ultrasound power, and when the ultrasound power was too high (320 W), the secondary structure of proteins became unstable.

### 3.8. Statistical analyses

The obtained experimental data were normalized, and correlation analysis was carried out. Fig. 6(a) shows the correlation heat map of thawing method and thawing index. It can be seen that relative to the DT group, the PT group had the largest positive correlation coefficient between WHC and protein ordered structure, and the smallest negative correlation coefficient between MDA and protein disordered structure, indicating that the beef had the best WHC, the smallest degree of lipid oxidation, and the most stable protein structure under this condition; the largest negative correlation coefficient between the number of colonies of the samples and media in the UPT group indicates that this condition has the strongest bactericidal ability; the positive correlation coefficient of thawing rate was the largest in the UDT and UPT groups, indicating that the intervention of ultrasound shortened the time of thawing, the negative correlation coefficient of ΔE was the largest in the PT and UPT groups, indicating that the PAW had a significant effect on maintaining the color of the beef. Fig. 6(b) shows the radar charts of each group, analyzed in terms of the area enclosed by each group, the UPT group was significantly larger than the UDT group, indicating that replacing the thawing medium with PAW significantly increased the quality of beef

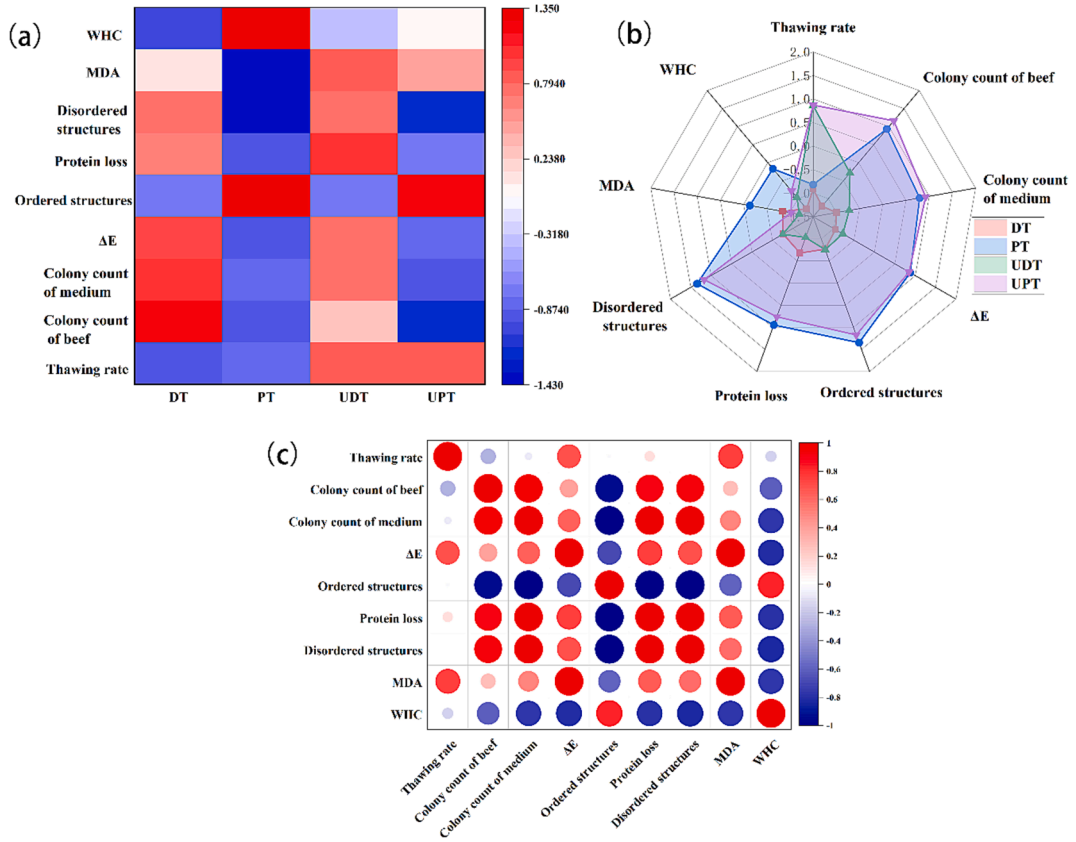


**Fig. 6. .** Statistical analysis. (a) Correlation heatmap of the thawing method and thawing index, (b) Radar map, (c) Pearson correlation coefficient matrix. **Note:** DT: deionized water thawing; PT: plasma-activated water thawing; UDT: ultrasound combined with deionized water thawing; UPT: ultrasound combined with plasma-activated water thawing.

after thawing. Fig. 6(c) is the Pearson correlation coefficient matrix showing the correlation between the different indicators. Thawing rate was positively correlated with ΔE and MDA content, indicating that thawing rate affects the color and lipid oxidation of the material after thawing. While MDA content showed a negative correlation with WHC, indicating that lipid oxidation would lead to a decrease in water holding capacity of beef after thawing. Meanwhile, the WHC after thawing was also related to the protein structure, which was positively correlated with the ordered structure of proteins and negatively correlated with the disordered structure. This research provides a theoretical and experimental basis for exploring the mechanism of PAW combined with ultrasound thawing technology on the WHC of beef.

## 4. Conclusion

In this research, PAW was used as a novel thawing medium combined with ultrasound to thaw beef. Compared with other thawing methods, the intervention of ultrasound significantly accelerated the thawing rate (38 % higher compared to the PT group), and the combination with PAW could effectively control the bacteria in beef and its culture medium (75 % higher compared to the UDT group), with no adverse effect on the color and pH value of beef. Meanwhile, based on the experimental results of drip loss, cooking loss, centrifugal loss and soluble matter loss, it was found that PAW could maintain the fiber structure of beef, improve its water holding capacity, better mitigate lipid oxidation of meat and reduce protein loss. In addition, protein structure analysis shows that PAW treatment can increase the ordered structure of proteins and stabilize their structure. Therefore, the feasibility of ultrasound combined with PAW in the field of meat thawing was proved, and the theoretical basis and experimental verification were provided for the wide application in the field of meat thawing.

## CRediT authorship contribution statement

**Huixin Wang:** Writing – review & editing, Writing – original draft, Visualization, Validation, Supervision, Software, Resources, Project administration, Methodology, Investigation, Funding acquisition, Formal analysis, Data curation, Conceptualization. **Changjiang Ding:** Writing – review & editing, Supervision, Investigation, Formal analysis. **Jingli Lu:** Supervision, Investigation, Formal analysis. **Yuting Bao:** Validation, Investigation. **Bingyang Han:** Validation, Data curation. **Jie Zhang:** Resources. **Shanshan Duan:** Software. **Zhiqing Song:** Methodology, Conceptualization. **Hao Chen:** Conceptualization.

## Declaration of competing interest

The authors declare that they have no known competing financial interests or personal relationships that could have appeared to influence the work reported in this paper.

## Data availability

No data was used for the research described in the article.

## Acknowledgements

This research was funded by National Natural Science Foundations of China (Nos. 52067017, 12365023 and 12265021), Program for Young Talents of Science and Technology in Universities of Inner Mongolia Autonomous Region of China (No. NJYT23020), Natural Science Foundation of Inner Mongolia Autonomous Region of China (Nos. 2022LHMS01002 and 2023LHMS05019), The Basic Scientific Research Business Project of the Universities Directly of the Inner Mongolia Autonomous Region (Nos. JY20220066 and JY20220232).

## References

Becton, M., Averett, R., & Wang, X. (2017). Effects of nanobubble collapse on cell membrane integrity. *J Micromech Mol Phys, 2*(2). https://doi.org/10.1142/s2424913017500084

Bian, C., Cheng, H., Yu, H., Mei, J., & Xie, J. (2022). Effect of multi-frequency ultrasound assisted thawing on the quality of large yellow croaker (Larimichthys crocea). *Ultrason. Sonochem., 82*, Article 105907. https://doi.org/10.1016/j.ultsonch.2021.105907

Cai, L., Zhang, W., Cao, A., Cao, M., & Li, J. (2019). Effects of ultrasonics combined with far infrared or microwave thawing on protein denaturation and moisture migration of Sciaenops ocellatus (red drum). *Ultrason Sonochem, 55*, 96–104. https://doi.org/10.1016/j.ultsonch.2019.03.017

Cai, L., Zhang, W., Cao, A., & Cao, M. (2020). Effects of different thawing methods on the quality of largemouth bass (Micropterus salmonides). *LWT Food Sci. Technol., 120*. https://doi.org/10.1016/j.lwt.2019.108908

Candoğan, K., Altuntas, E. G., & İğci, N. (2020). Authentication and quality assessment of meat products by fourier-transform infrared (FTIR) spectroscopy. *Food Eng. Rev., 13*(1), 66–91. https://doi.org/10.1007/s12393-020-09251-y

Cao, S., Hu, Z., Pang, B., Wang, H., Xie, H., & Wu, F. (2010). Effect of ultrasound treatment on fruit decay and quality maintenance in strawberry after harvest. *Food Control, 21*(4), 529–532. https://doi.org/10.1016/j.foodcont.2009.08.002

Carbonaro, M., Maselli, P., & Nucara, A. (2012). Relationship between digestibility and secondary structure of raw and thermally treated legume proteins: A Fourier transform infrared (FT-IR) spectroscopic study. *Amino Acids, 43*(2), 911–921. https://doi.org/10.1007/s00726-011-1151-4

Chaijan, M., Chaijan, S., Panya, A., Nisoa, M., Cheong, L.-Z., & Panpipat, W. (2021). High hydrogen peroxide concentration-low exposure time of plasma-activated water (PAW): A novel approach for shelf-life extension of Asian sea bass (Lates calcarifer) steak. *Innov. Food Sci. Emerg. Technol., 74*, Article 102861. https://doi.org/10.1016/j.ifset.2021.102861

Coombs, C. E., Holman, B. W., Friend, M. A., & Hopkins, D. L. (2017). Long-term red meat preservation using chilled and frozen storage combinations: A review. *Meat Sci., 125*(1), 84–94. https://doi.org/10.1016/j.meatsci.2016.11.025

Dominguez, R., Pateiro, M., Gagaoua, M., Barba, F. J., Zhang, W., & Lorenzo, J. M. (2019). A comprehensive review on lipid oxidation in meat and meat products. *Antioxidants (Basel), 8*(10), 429. https://doi.org/10.3390/antiox8100429

Eastridge, J. S., & Bowker, B. C. (2011). Effect of rapid thawing on the meat quality attributes of USDA select beef strip loin steaks. *J. Food Sci., 76*(2), 156–162. https://doi.org/10.1111/j.1750-3841.2010.02037.x

Forghani, F., & Oh, D. H. (2013). Hurdle enhancement of slightly acidic electrolyzed water antimicrobial efficacy on Chinese cabbage, lettuce, sesame leaf and spinach using ultrasonication and water wash. *Food Microbiol, 36*(1), 40–45. https://doi.org/10.1016/j.fm.2013.04.002

Gambuteanu, & Alexe., C. a. P. (2013). Effects of ultrasound assisted thawing on microbiological, chemical and technological properties of unpackaged pork Longissimus dorsi. Annals of the University Dunarea De Jos of Galati, 37(1), 98-107.

Ganesan, A. R., Tiwari, U., Ezhilarasi, P. N., & Rajauria, G. (2021). Application of cold plasma on food matrices: A review on current and future prospects. *J. Food Process. Preserv., 45*(1), 15070. https://doi.org/ARTN e1507010.1111/jfpp.15070.

Gan, S., Zhang, M., Mujumdar, A. S., & Jiang, Q. (2022). Effects of different thawing methods on quality of unfrozen meats. *Int. J. Refrig, 134*, 168–175. https://doi.org/10.1016/j.ijrefrig.2021.11.030

Han, B., Ding, C., Jia, Y., Wang, H., Bao, Y., Zhang, J., & Lu, J. (2023). Influence of electrohydrodynamics on the drying characteristics and physicochemical properties of garlic. *Food Chemistry: X, 19*, Article 100818. https://doi.org/10.1016/j.fochx.2023.100818

Herianto, S., Shih, M.-K., Lin, C.-M., Hung, Y.-C., Hsieh, C.-W., Wu, J.-S., & Hou, C.-Y. (2022). The effects of glazing with plasma-activated water generated by a piezoelectric direct discharge plasma system on whiteleg shrimp (Litopenaeus vannamei). *LWT Food Sci. Technol., 154*, Article 112547. https://doi.org/10.1016/j.lwt.2021.112547

Hsieh, C. W., Lai, C. H., Ho, W. J., Huang, S. C., & Ko, W. C. (2010). Effect of thawing and cold storage on frozen chicken thigh meat quality by high-voltage electrostatic field. *J. Food Sci., 75*(4), 193–197. https://doi.org/10.1111/j.1750-3841.2010.01594.x

Huff-Lonergan, E., & Lonergan, S. M. (2005). Mechanisms of water-holding capacity of meat: The role of postmortem biochemical and structural changes. *Meat Sci., 71*(1), 194–204. https://doi.org/10.1016/j.meatsci.2005.04.022

Islam, M. N., Zhang, M., Adhikari, B., Xinfeng, C., & Xu, B.-G. (2014). The effect of ultrasound-assisted immersion freezing on selected physicochemical properties of mushrooms. *Int. J. Refrig, 42*, 121–133. https://doi.org/10.1016/j.ijrefrig.2014.02.012

Jo, K., Lee, S., Yong, H. I., Choi, Y.-S., & Jung, S. (2020). Nitrite sources for cured meat products. *LWT Food Sci. Technol., 129*, Article 109583. https://doi.org/10.1016/j.lwt.2020.109583

Kong, D., Quan, C., Xi, Q., Han, R., Koseki, S., Li, P., & Wang, J. (2022). Study on the quality and myofibrillar protein structure of chicken breasts during thawing of ultrasound-assisted slightly acidic electrolyzed water (SAEW). *Ultrason. Sonochem., 88*, Article 106105. https://doi.org/10.1016/j.ultsonch.2022.106105

Li, D., Zhao, H., Muhammad, A. I., Song, L., Guo, M., & Liu, D. (2020). The comparison of ultrasound-assisted thawing, air thawing and water immersion thawing on the quality of slow/fast freezing bighead carp (Aristichthys nobilis) fillets. *Food Chem., 320*, Article 126614. https://doi.org/10.1016/j.foodchem.2020.126614

Li, H., Wang, L., Wang, J., Li, X., Li, J., Cui, F., & Mi, H. (2023). Effects of ultrasound-assisted freezing on the quality of large yellow croaker (Pseudosciaena crocea)

subjected to multiple freeze-thaw cycles. *Food Chem., 404*(Pt A), Article 134530. https://doi.org/10.1016/j.foodchem.2022.134530

Li, X. x., Ma, Y., Sun, P., Liu, H., Cai, L., & Li, J. r. (2020). Effect of ultrasonic thawing on protein properties and muscle quality of Bonito. Journal of Food Processing and Preservation, 45(1), 14930. https://doi.org/10.1111/jfpp.14930.

Li, Y., Song, Z., Zhang, T., Ding, C., & Chen, H. (2022). Gene expression variation of Astragalus adsurgens Pall. through discharge plasma and its activated water. *Free Radic. Biol. Med., 182*, 1–10. https://doi.org/10.1016/j.freeradbiomed.2022.02.016

Liu, D., Liang, L., Xia, W., Regenstein, J. M., & Zhou, P. (2013). Biochemical and physical changes of grass carp (Ctenopharyngodon idella) fillets stored at -3 and 0 degrees C. *Food Chem., 140*(1–2), 105–114. https://doi.org/10.1016/j.foodchem.2013.02.034

Lu, X., Jiang, Z., Xiong, Q., Tang, Z., Hu, X., & Pan, Y. (2008). An 11cm long atmospheric pressure cold plasma plume for applications of plasma medicine. *Appl. Phys. Lett., 92*(8), Article 081502. https://doi.org/10.1063/1.2883945

Pang, B., Bowker, B., Zhuang, H., Yang, Y., & Zhang, J. (2020). Research Note: Comparison of 3 methods used for estimating cook loss in broiler breast meat. *Poult. Sci., 99*(11), 6287–6290. https://doi.org/10.1016/j.psj.2020.08.038

Qian, J., Yan, L., Ying, K., Luo, J., Zhuang, H., & Yan, W. (2022). Plasma-activated water: A novel frozen meat thawing media for reducing microbial contamination on chicken and improving the characteristics of protein. *Food Chem., 375*, Article 131661. https://doi.org/10.1016/j.foodchem.2021.131661

Qian, S., Li, X., Wang, H., Mehmood, W., Zhong, M., Zhang, C., & Blecker, C. (2019). Effects of low voltage electrostatic field thawing on the changes in physicochemical properties of myofibrillar proteins of bovine Longissimus dorsi muscle. *J. Food Eng., 261*, 140–149. https://doi.org/10.1016/j.jfoodeng.2019.06.013

Rossow, M., Ludewig, M., & Braun, P. G. (2018). Effect of cold atmospheric pressure plasma treatment on inactivation of Campylobacter jejuni on chicken skin and breast fillet. *LWT Food Sci. Technol., 91*, 265–270. https://doi.org/10.1016/j.lwt.2018.01.052

Royintarat, T., & Seesuriyachan, P. (2019). Mechanism and optimization of non-thermal plasma-activated water for bacterial inactivation by underwater plasma jet and delivery of reactive species underwater by cylindrical DBD plasma. *Curr. Appl Phys., 19*(9), 1006–1014. https://doi.org/10.1016/j.cap.2019.05.020

Sriket, P., Benjakul, S., Visessanguan, W., & Kijroongrojana, K. (2007). Comparative studies on the effect of the freeze–thawing process on the physicochemical properties and microstructures of black tiger shrimp (Penaeus monodon) and white shrimp (Penaeus vannamei) muscle. *Food Chem., 104*(1), 113–121. https://doi.org/10.1016/j.foodchem.2006.11.004

Vinarov, D. A., Lytle, B. L., Peterson, F. C., Tyler, E. M., Volkman, B. F., & Markley, J. L. (2004). Cell-free protein production and labeling protocol for NMR-based structural proteomics. *Nat. Methods, 1*(2), 149–153. https://doi.org/10.1038/nmeth716

Wang, B., Bai, X., Du, X., Pan, N., Shi, S., & Xia, X. (2022). Comparison of effects from ultrasound thawing, vacuum thawing and microwave thawing on the quality properties and oxidation of porcine longissimus lumborum. *Foods, 11*(9), 11091368. https://doi.org/10.3390/foods11091368

Xu, B.-G., Zhang, M., Bhandari, B., Cheng, X.-F., & Sun, J. (2015). Effect of ultrasound immersion freezing on the quality attributes and water distributions of wrapped red radish. *Food Bioproc. Tech., 8*(6), 1366–1376. https://doi.org/10.1007/s11947-015-1496-x

Xu, Y., Tian, Y., Ma, R., Liu, Q., & Zhang, J. (2016). Effect of plasma activated water on the postharvest quality of button mushrooms. *Agaricus bisporus. Food Chemistry, 197*(Pt A), 436–444. https://doi.org/10.1016/j.foodchem.2015.10.144

Zhang, M., Haili, N., Chen, Q., Xia, X., & Kong, B. (2018). Influence of ultrasound-assisted immersion freezing on the freezing rate and quality of porcine longissimus muscles. *Meat Sci., 136*, 1–8. https://doi.org/10.1016/j.meatsci.2017.10.005

Zhang, Y. M., Ding, C. J., Ni, J. B., Song, Z. Q., & Zhao, R. (2019). Effects of high-voltage electric field process parameters on the water-holding capacity of frozen beef during thawing process. *Journal of Food Quality, 2019*, 9140179. https://doi.org/Artn 914017910.1155/2019/9140179.

Zhang, Z., Yang, Y., Zhou, P., Zhang, X., & Wang, J. (2017). Effects of high pressure modification on conformation and gelation properties of myofibrillar protein. *Food Chem., 217*, 678–686. https://doi.org/10.1016/j.foodchem.2016.09.040